*IEIE Transactions on Smart Processing and Computing, vol. 4, no. 5, October 2015*
http://dx.doi.org/10.5573/IEIESPC.2015.4.5.297



# Test of a Multilayer Dose-Verification Gaseous Detector with Raster-Scan-Mode Proton Beams

**Kyong Sei Lee[1†], Sung Hwan Ahn[2*] , Youngyih Han[2], Byungsik Hong[1], Sang Yeol Kim[3], and Sung Keun Park[1]**

[1] Department of Physics, Korea University, Seoul 02841 (kslee0421@korea.ac.kr)
[2] Department of Radiation Oncology, Samsung Medical Center, Seoul 06351
[3] Notice Korea, Anyang 14088

† Corresponding Author: Kyong Sei Lee

***** Contributed equally to this work.

*Received October 7, 2015; Revised October 15, 2015; Accepted October 20, 2015; Published October 31, 2015*

** Regular Paper*

***Abstract*:** A multilayer gaseous detector has been developed for fast dose-verification measurements of raster-scan-mode therapeutic beams in particle therapy. The detector, which was constructed with eight thin parallel-plate ionization chambers (PPICs) and polymethyl methacrylate (PMMA) absorber plates, is closely tissue-equivalent in a beam's eye view. The gas-electron signals, collected on the strips and pad arrays of each PPIC, were amplified and processed with a continuous charge–integration mode. The detector was tested with 190-MeV raster-scan-mode beams that were provided by the Proton Therapy Facility at Samsung Medical Center, Seoul, South Korea. The detector responses of the PPICs for a 190-MeV raster-scan-mode proton beam agreed well with the dose data, measured using a 2D ionization chamber array (Octavius model, PTW). Furthermore, in this study it was confirmed that the detector simultaneously tracked the doses induced at the PPICs by the fast-oscillating beam, with a scanning speed of 2 m s-1. Thus, it is anticipated that the present detector, composed of thin PPICs and operating in charge–integration mode, will allow medical scientists to perform reliable fast dose-verification measurements for typical dynamic mode therapeutic beams.

***Keywords*:** Particle therapy, Parallel plate ionization chambers, Dose verification, Raster-scan-mode proton beam

## 1. Introduction

In radiation therapy, proton [1-5] and heavy-ion beams [6-10] have a great advantage over X-rays because of the high radiation biological effectiveness (RBE) of inflicting biological damage on malignant tumors and also of suppressing fast recovery of the DNA. Furthermore, the well-controlled delivery of the radiation dose to the planned treatment volume (PTV) by using Bragg peaks, and the well-defined depth of interaction, minimizes unnecessary delivery of the dose to normal tissue or sensitive organs surrounding the cancer tumor. As particle therapy technology becomes more sophisticated, it is necessary to have more accurate and swifter confirmation of the proper measurement, and verification of the doses to be delivered to patients.

In particle therapy, the wire chambers operating in ionization-chamber mode have typically been used to monitor beams and for precise dose-verification measurements [9]. The detector responses, which have to be interpreted for the dose rate and to confirm the beam, are measured in the two coordinates vertical to the beam direction and as functions of the depth of interaction in a water phantom, by consecutively changing the thickness of the water lying in front of the detector surface. Furthermore, the ionization-chamber-mode gaseous detectors allow us to avoid the complicated correction procedure [11] for nonlinear detector response to specific energy loss of the baryonic particles [12], which would be critical when organic-scintillator-based detectors are utilized for verification of the therapeutic beam.

Simultaneous measurement over the whole depth range will be fairly conducive to reducing both scan time and the labor required for the dose verification process. Tracking

the movement of the fast oscillating dynamic-mode beams would also be advantageous in verifying whether each component of the beam is correctly delivered at all depth positions in the PTV as planned.

## 2. Construction of the Detector

The gaseous detector for particle therapy dose verification, which was developed in the present research, is briefly summarized as follows.

(1) The detector is composed of eight thin and uniform parallel-plate ionization chambers (PPICs) where signals are collected by fine strips and pad arrays with a pitch of 1.25 mm.

(2) The mean material density of the detector that the therapeutic beams experienced was closely adjusted to be tissue equivalent (1.003 g·cm$^{-3}$) [13] in a beam's eye view, within an accuracy of about 0.15% (standard deviation).

(3) The detector response data are processed by amplifying and integrating the gas-electron signals over continuous system clock-time intervals of 28.6 μs.

(4) The detector response data are reconstructed every 228.6 μs, which allows for reproduction of a maximum 8×4372 frames per second of dose images.

The multilayer gaseous detector in the present research and development was designed for dose verification of therapeutic proton beams with a maximum energy of 200 MeV, where the predicted distal edge in the detector is 27 g·cm$^{-2}$. The detector was assembled with eight-layer interlaced thin PPICs and absorbers made of polymethyl methacrylate (PMMA) plates (see Fig. 1). The mean density of the detector that therapeutic particles experience was closely adjusted to 1.003 g·cm$^{-3}$ by properly placing the PMMA plates with thicknesses of 5 mm and 10 mm. The size of the gap lying between two adjacent PPICs, allowing the placing of the PMMA plates, was adjusted to 3.6 g·cm$^{-2}$.

To achieve a complete three-dimensional measurement with high voxel granularity, additional PMMA absorber plates can be placed anterior to the front surface of the detector. For example, the scan measurements for the designed beam can be repeated with absorber thicknesses increasing from 0 to 3.2 g·cm$^{-2}$, in 0.4 g·cm$^{-2}$ steps. Then, there is reconstruction of a complete set of data with the desired voxel granularity, with a total of 72 depth steps in the beam direction. The amount of time required to complete a single dose-verification measurement with a 10-s scan measurement for each step was expected to be less than 300 s. The single 10-s beam to be measured at each step may contain many beam components with different energies, which are required to properly cover the tumor size.

The structure of a PPIC designed in the present research is illustrated with a schematic diagram in the top half of Fig. 2. The thickness of the induction region, formed between the cathode and the signal planes, was adjusted to 3.8 mm. The copper patterns for the cathode and signal planes were printed on 1.6-mm thick printed circuit boards (PCBs). The signal plane is composed of

**Fig. 1. Gaseous detector constructed with eight-layer interlaced thin PPICs and absorbers made of PMMA plates.**

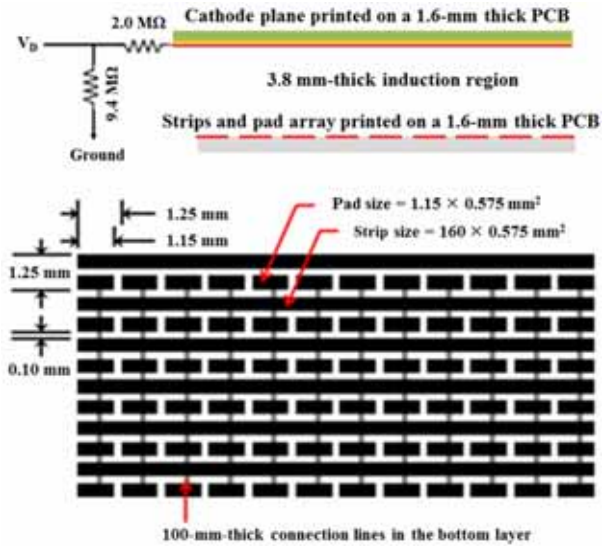


**Fig. 2. Copper pattern for the signal plane composed of 1.25-mm-pitch strips and pad arrays printed on the top layer of a 1.6-mm-thick PCB. The 100-μm-wide traces required for the electrical connections for the pads were printed on the bottom layer of the PCB.**

1.25-mm-pitch strips and pad arrays, printed on the top layer of the PCB, as can be seen in the bottom half of Fig. 2. The strips and the pad arrays, 128 of each, were assigned to measure the separate detector responses in the vertical ($y$) and horizontal ($x$) directions, respectively. The 100-μm-wide traces, required for the electrical connections for the pad arrays, were printed on the bottom layer.

The typical electrical potential of –570 V, applied to the cathode plane, provides a uniform electric field intensity of 1.5 kV cm$^{-1}$ in the induction volume of the PPIC. It was shown in previous research [14, 15] that amplification of the gas electrons was fairly insignificant, over the wide range of electric-field intensity, when the present ionization-mode detector was operated with a gas mixture of 70% Ar + 30% $CO_2$.

The 256-channel electronics board for the signal process and the data transfer, each assigned to a PPIC, was

**Fig. 3. Detector installed at a distance of 10 cm from the rectangular copper collimator, mounted in the rotating beam gantry, where a compensation Bolus, required to further focus the dose to the patient's tumor, is to be placed.**

composed of four 64-channel charge integrators, eight amplifiers, an eight-channel analog-to-digital converter processor, a field programmable gate array (FPGA) digital processor, and a USB3 interface processor. The details for this electronics design are described in previous reports [16, 17].

The gas-electron signals collected in the strips and pad arrays of the detectors were integrated every 28.6 μs and converted to the integrated charge values (channel responses). The maximum sensitivity of the proton-induced current per channel was adjusted to 20 nA.

## 3. Tests of the detector with raster-scan-mode proton beams

The performance of the present dose-verification detector was examined with 190-MeV raster-scan-mode beams that were provided by the Proton Cyclotron Facility at the Samsung Medical Center, Seoul, South Korea. The detector was installed at a distance of 10 cm from the rectangular copper collimator, mounted in the rotating beam gantry, where a compensation Bolus, which is required to further focus the dose to the patient's tumor, is to be placed (see Fig. 3).

A schematic of a typical raster scan, with a thin pencil-shaped pristine proton beam, can be seen in Fig. 4. The blue line indicates the passage of the Bragg peak of a monoenergetic beam on the surface, lying at a set depth in the PTV. The depth of a scan in the PTV can be adjusted by changing the energy of the beam.

In Fig. 5, the time responses are shown for the first PPIC for a 1.0-nA 190-MeV raster-scan-mode proton beam with a scanning speed of 10 m $s^{-1}$, measured by the pad arrays ($x$), seen in the top panel, and the strips ($y$), seen in the bottom panel, for a 1-s period. The field size of the

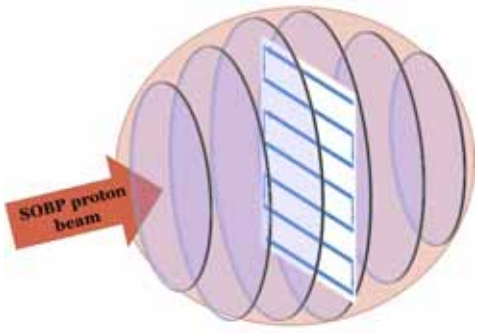


**Fig. 4. Typical raster scan with thin pencil-shaped pristine proton beams. The blue line indicates the passage of the Bragg peak of a monoenergetic beam on the surface lying at a set depth in the PTV.**

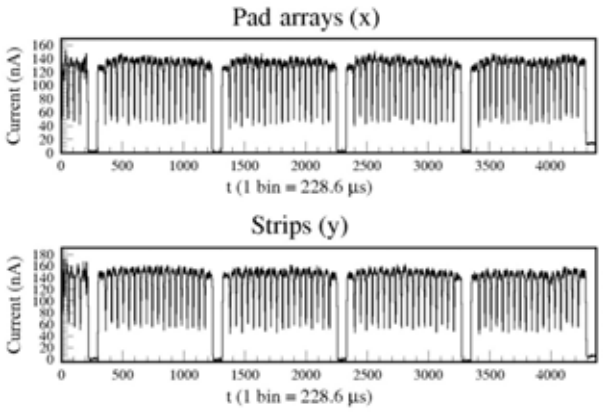


**Fig. 5. Time responses of the first PPIC to the raster-scan-mode beam for 1 s measured by pad arrays (*x*), top panel, and strips (*y*), bottom panel.**

beam was adjusted to 11 × 11 $cm^2$. The substructures of the time profiles in Fig. 5 respect the movement of the beam in the detector, equivalent to a PTV, as illustrated in Fig. 4. The required duration for completion of a single raster scan was measured as 233 ms.

The procedure of the fast oscillating raster-scan-mode beam, which induces the dose at each depth in the detector phantom, can be visualized in pseudo-two-dimensional images where the data, obtained by multiplying the channel-response functions in the x and the y directions (*i.e.*, $F(x,y)=\sqrt{f(x)\times f(y)}$) are sequentially added. Fig. 6 shows the pseudo-2D images for the raster-scan-mode beam, as measured at the first PPIC at 0.014 s (top left), 0.048 s (top middle), 0.128 s (top right), 0.256 s (bottom left), 1 s (bottom middle), and 10 s (bottom right), after the start of the measurement. The width (full width at half maximum) of the raster-scan-mode beam measured about 14 mm (see Fig. 6). As shown in the bottom-right pseudo-2D image in Fig. 6, the flatness of the proton field, measured for 10 s, is fairly satisfactory for achieving the accuracy required for the precision radiological operation. The movement of the beam in the raster-scan motion, measured at the first PPIC for the first 48 ms, can be seen in the pseudo-2D images (Fig. 7). They are fairly

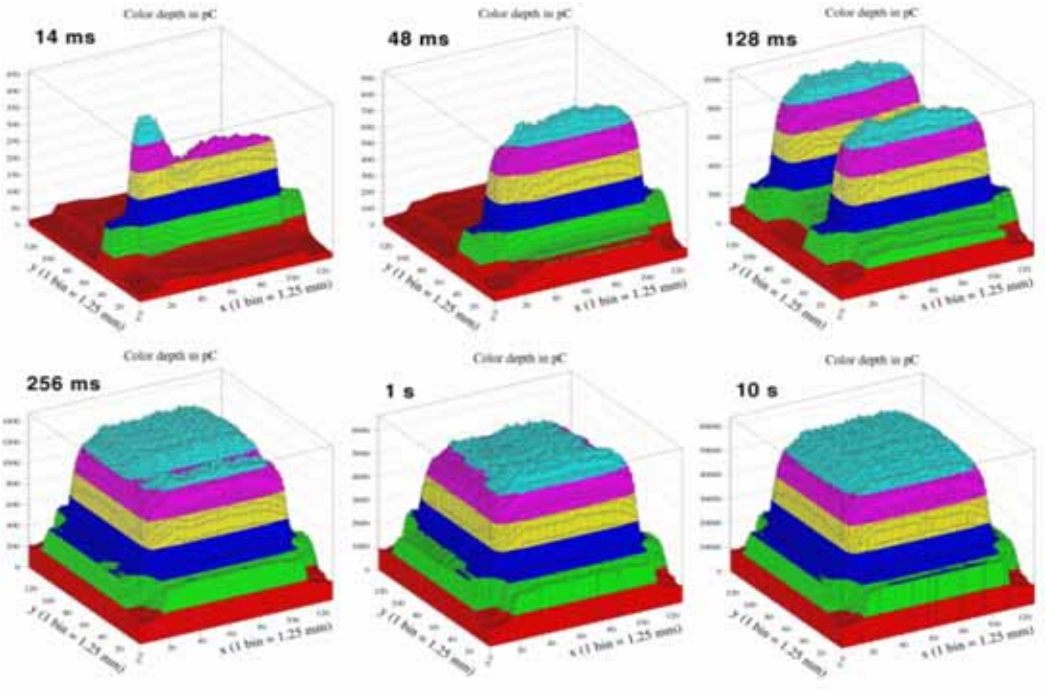


**Fig. 6. Pseudo-2D images for the raster-scan-mode beam measured at the first PPIC at 0.014 s (top left), 0.048 s (top middle), 0.128 s (top right), 0.256 s (bottom left), 1 s (bottom middle), and 10 s (bottom right) after the start of the measurement.**

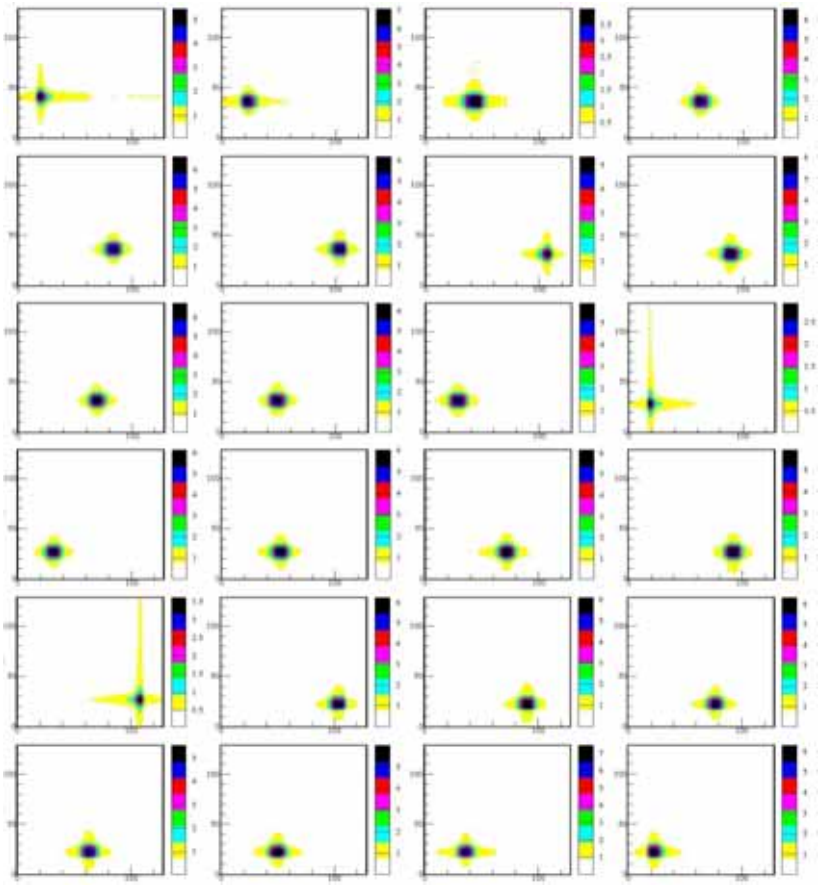

**Fig. 7. Movement of the beam in the raster-scan motion measured by the first PPIC for first 48 ms.**

conducive to the precision space–time analysis and the relevant visualization for the rapidly oscillating dynamic mode beam.

Fig. 8 shows total detector responses (full circles) of

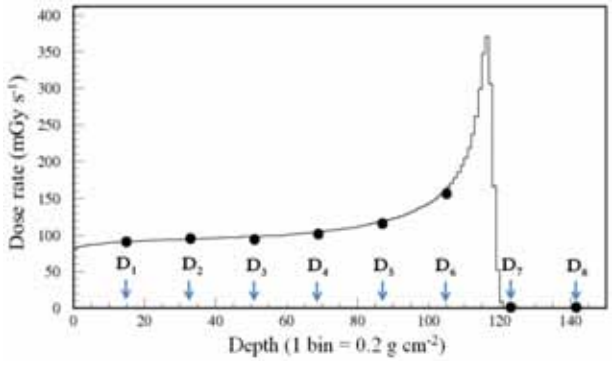


**Fig. 8. Total detector responses (full circles) of the PPICs, denoted by "$D_i$," with *i* ranging from 1 to 7, and installed at the first seven depths in the tissue-equivalent detector to a 1.6-nA 190-MeV raster-scan-mode proton beam for 2.4 s and a scanning speed of 2 m $s^{-1}$.**

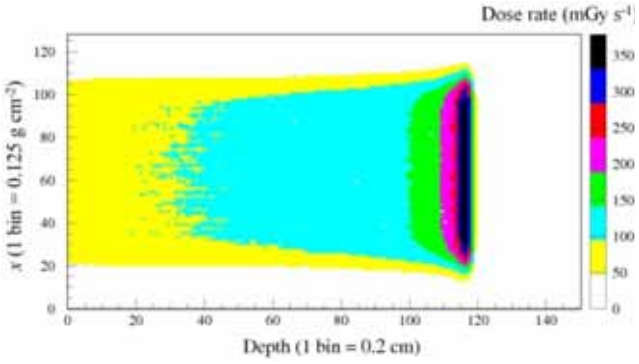


**Fig. 9. Two-dimensional representation of the dose simulated by the GEANT4 program as a function of the depth and one direction perpendicular to the depth direction.**

the PPICs denoted by "$D_i$," with *i* ranging from 1 to 7, and installed at the first seven depths in the tissue-equivalent detector of a 1.6-nA 190-MeV raster-scan-mode proton beam, with a duration of 2.4 s and a scanning speed of 2 m $s^{-1}$. The field size of the beam was adjusted to 10 × 10 $cm^2$. The solid curve in Fig. 8 is the one-dimensional Bragg curve that was predicted by performing a GEANT4 simulation [18-20]. The positions of the Bragg peak and the distal edge of the 190-MeV protons are expected to be 23.3 g·$cm^{-2}$ and 24.0 g·$cm^{-2}$, respectively. For the proper comparison of the data with the Bragg curve obtained by the GEANT4 simulation, the relative strengths of the PPIC responses were adjusted by normalizing the first detector response (denoted by "$D_1$") to the simulated dose rate at the same depth. Fig. 9 shows a two-dimensional representation of the dose simulated by the GEANT4 program as a function of the depth and one direction perpendicular to the depth direction. The width of the area of the 190-MeV raster-scan-mode beam becomes broader by about 15% as the beam reaches the Bragg peak.

The distributions of the detector responses of the eight PPICs in the *x* and the *y* directions for the 1.6-nA 190 MeV raster-scan-mode proton beam are shown in the first and second columns, respectively, in Fig. 10. The relatively large statistical fluctuations of the distributions were attributed to the absence of proper calibrations for the channel sensitivities of the electronics, which will be properly performed using a raster-scan-mode beam where the field area is fairly flat and wider than the detector's active area. Nevertheless, the detector responses measured at the first seven depths, as shown in Figs. 8 and 10, coincided well with the simulated dose rates.

The figures in the third column of Fig. 10 show pseudo-2D images of the detector responses, measured for the 1.6-nA 190-MeV raster-scan-mode proton beam at the first seven depths. The pseudo-2D images illustrate how the area of the radiation field and the relative strength increase as the depth increases (see Fig. 10). However, it should be noted that the strength near the periphery of the radiation field (the halo) is inevitably exaggerated, as shown in the pseudo-2D image that has been reconstructed by the multiplication of the two response functions. It is not equivalent to a "true" 2D image, unless the raster scan is performed using a beam with an infinitely narrow width. Thus, the use of the pseudo-2D images should be restricted to the confirmation of an area and the flatness of a radiation field, as well as verification of the movement of the beam in the detector.

The measurements performed by the present detector were confirmed by using a planar-type 2D-ionization chamber array (Octavius model, PTW). Fig. 11 shows a 2D image (left) and the 1D-horizontal distribution (right) for 1 s for a raster-scan-mode beam of the same energy and field area as the one visualized in Fig. 10. Except for the inevitable enhancement of the strengths near the peripheries, the flatness of the central region and the thickness of the halo measured at each depth by the present detector agree well with those shown in Fig. 11. Fig. 12 shows the 1D dose distribution (Bragg curve) for the 190-MeV raster-scan-mode beam measured using a detector composed of 180 PPICs (ZEBRA model, IBA). The positions of the Bragg peak and the distal edge for the 190-MeV protons also agree well with the simulation data performed by the GEANT4 program (Fig. 8).

## 4. Conclusion

In this study, we constructed a gaseous detector composed of multilayer PPICs and PMMA absorbers, and examined a proposed radiation technique for fast particle therapy dose verification by using therapeutic proton beams provided by the Proton Therapy Facility at the Samsung Medical Center, Seoul, South Korea. The prototype detector was manufactured to be closely tissue equivalent in a beam's eye view. The performance of the prototype detector was confirmed using raster-scan-mode proton beams, where the energy, field area, scan speed, and pattern are typically used in dynamic mode treatments. The conclusions of the present research, performed with the prototype detector, are summarized as follows.

(1) The flatness of a radiation field of a raster-scan-

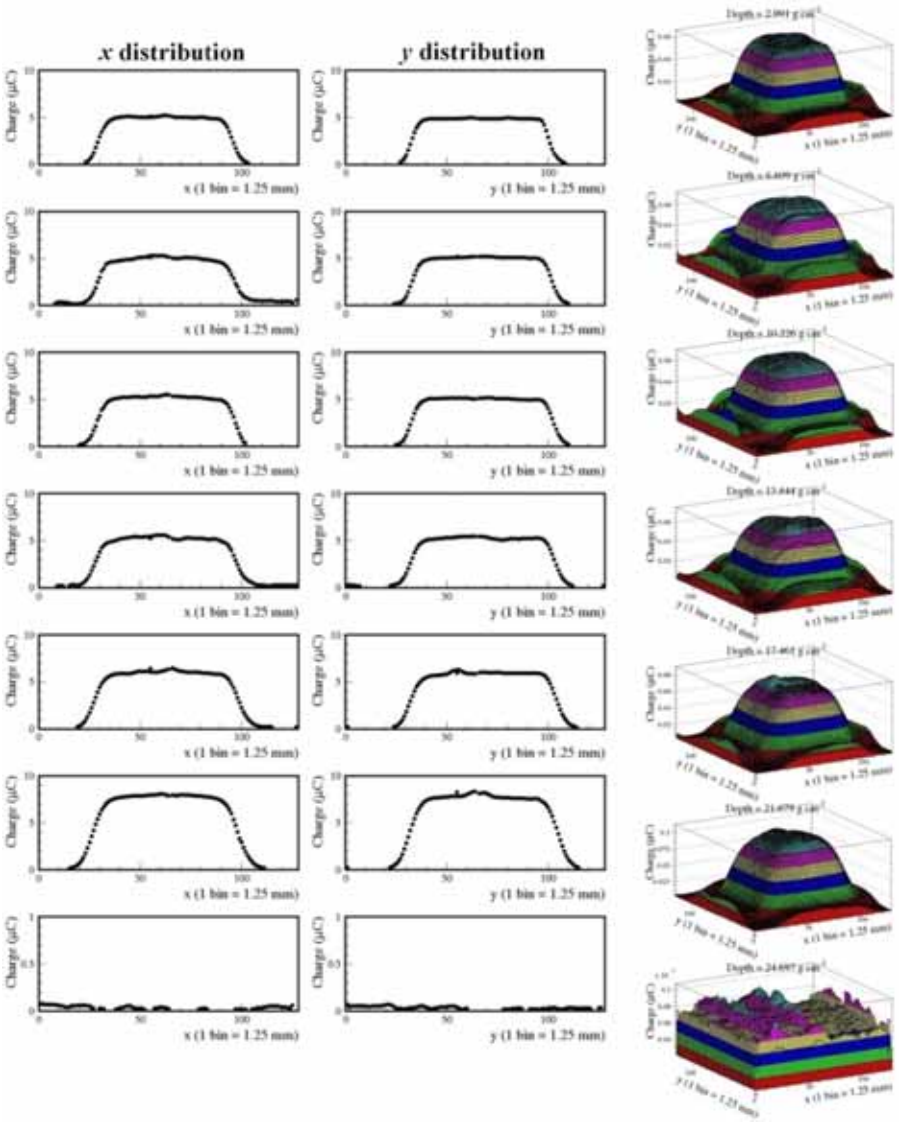


**Fig. 10. Distributions of the detector responses of the first seven PPICs in the *x* (first column) and the *y* (second column) directions for the 1.6-nA 190-MeV raster-scan-mode beam. The corresponding pseudo-2D images are shown in the third column.**

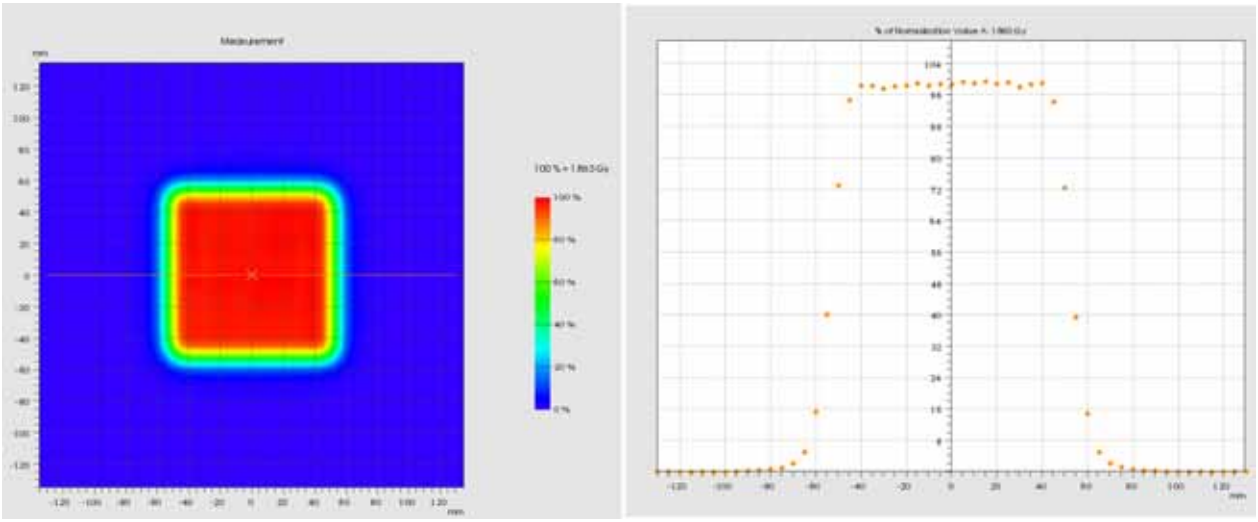

**Fig. 11. 2D image (left) and the 1D horizontal dis-tribution (right) for a 1.6-nA 190-MeV raster-scan-mode beam measured using a planar-type 2D ionization chamber array (Octavius model, PTW) for 1 s.**

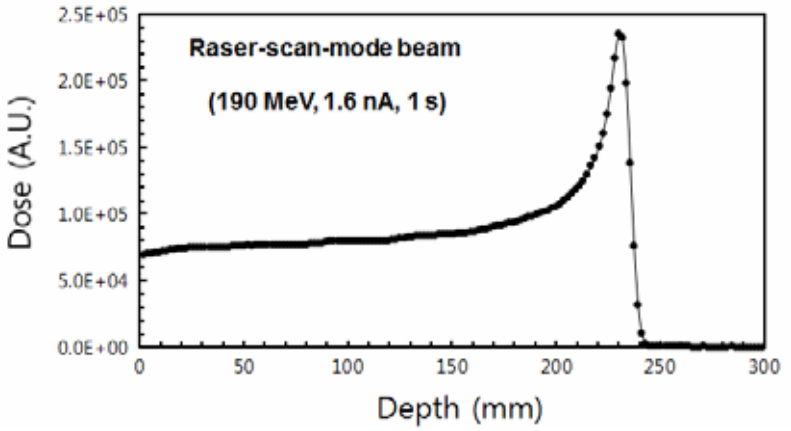


**Fig. 12. 1D dose distribution (Bragg curve) for the 190-MeV raster-scan-mode beam measured using a detector composed of 180 PPICs (ZEBRA model, IBA).**

mode proton beam, provided by the Proton Therapy Facility (Samsung Medical Center Seoul, South Korea) is fairly satisfactory for achieving the accuracy required for a precision radiological particle therapy operation.

(2) The movements of the fast raster-scan motion of the beam in the detector system were reproduced well in the pseudo-2D images that were reconstructed from the data and time responses. They will be fairly conducive to a precision analysis and a proper visualization in clinical procedures with dynamic mode therapeutic beams.

(3) The detector responses of the PPICs, placed in the detector, coincide well with the dose rates predicted by the GEANT4 code.

The development of detailed clinical procedures for dose verification is a future research task with the present detector. They will include proper procedures for calibration of channel sensitivities and for multi-step measurements to obtain voxel data that completely cover fine depth positions, as well as a critical evaluation of the performance of the detector when applied to the actual radiation treatment process. A promising new development for the detector would entail using the current research and development results of heavy-ion therapy, after construction of the first heavy ion medical facility is completed in the near future in Korea.

## Acknowledgement

This study was supported by the National Research Foundation of Korea (Grant Numbers NRF-2013R1A1 A2060257 and NRF-2013M2B2A9A-03050128).

## References

[1] C. Talamonti *et al*., Nucl. Instr. Meth. A **612** (2010) 571. Article (CrossRef Link)

[2] W. Wagner, M. Seidel, E. Morenzoni, F. Groeschel, M. Wohlmuther and M. Daum, Nucl. Instr. Meth. A **600** (2009) 5. Article (CrossRef Link)

[3] T. Bortfeld, Phys. Med. Biol. **51** (2006) R363. Article (CrossRef Link)

[4] H. Paganetti, H. Jiang, K. Parodi, R. Slopsema and M. Engelsman, Phys. Med. Biol. **53** (2008) 4825. Article (CrossRef Link)

[5] H. Paganetti, H. Jiang, J. A. Adams, G. T. Chen and E. Rietzel, Int. J. Radiat. Oncology Biol. Phys. **60** (2004) 942. Article (CrossRef Link)

[6] 'Technologies for delivery of proton and ion beams for radiotherapy', H. Owen, D. Holder, J. Alonso and R. Mackay, arXiv:1310.0237v1 Oct. 2013. Article (CrossRef Link)

[7] T. Inaniwa, T. Furukawa, S. Sato, T. Tomitani, M. Kobayashi, S. Minohara, K. Noda and T. Kanai, Nucl. Instr. Meth. B **266** (2007) 2194. Article (CrossRef Link)

[8] Y. Futami, T. Kanai, M. Fujita, H. Tomura, A. Higashi, N. Matsufuji, N. Miyahara, M. Endo and K. Kawachi, Nucl. Instr. Meth. A **430** (1999) 143. Article (CrossRef Link)

[9] K. Nada *et al*., J. Radiat. Res. **48**: Suppl. (2007) A43. Article (CrossRef Link)

[10] M. Torikoshi, K. Noda, E. Takada, T. Kanai, S. Yamada, H. Ogawa, K. Okumura, K. Narita, K. Ueda and M. Mizobata, Nucl. Instr. Meth. A **435** (1999) 326. Article (CrossRef Link)

[11] S. Lee, B. Hong, K. S. Lee, B. Mulilo and S. K. Park, Nucl. Instr. Meth. A **724** (2013) 6. Article (CrossRef Link)

[12] M. Hirschberg, R. Beckmann, U. Brandenburg, H. Bruckmann and K. Wick, IEEE Trans. Nucl. Sci. **39** (1992) 511. Article (CrossRef Link)

[13] The standard composition ratios of the constituent elements of soft tissue are found at http://pdg.lbl.gov/2012/AtomicNuclearProperties/.

[14] K. S. Lee, B. Hong, S. K. Park and S. Y. Kim, J. Korean Phys. Soc. **65** (2014) 1367. Article (CrossRef Link)

[15] K. S. Lee, B. Hong, K. Lee, S. K. Park and J. Yu, J. Korean Phys. Soc. **64** (2014) 958. Article (CrossRef Link)

[16] K. S. Lee, B. Hong, G. Jhang, M. Jo, E. Ju, B. S. Moon, S. K. Park, H. B. Rhee, H. H. Shim and K. S. Sim, J. Korean Phys. Soc. **59** (2011) 2002. Article (CrossRef Link)
[17] K. S. Lee, B. Hong, K. Lee, G. Jhang, E. Ju, C. Kim, S. K. Park, H. B. Rhee, H. H. Shim and K. S. Sim, J. Korean Phys. Soc. **58** (2011) 706. Article (CrossRef Link)
[18] K. S. Lee, B. Hong, S. K. Park and K. S. Sim, J. Korean Phys. Soc. **58** (2011) 15. Article (CrossRef Link)
[19] J. Allison *et al*., IEEE Trans. Nucl. Sci. **53** (2006) 270. Article (CrossRef Link)
[20] S. Agostinelli *et al*., Nucl. Instr. Meth. A **506** (2003) 250. Article (CrossRef Link)

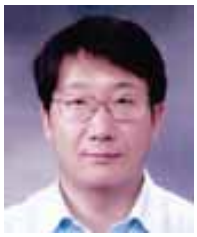

**Kyong Sei Lee** is a research professor of the Institute of Basic Sciences and Dept. of Physics at Korea University. He received his B.S. and M.S. degrees in physics and nuclear physics at Korea University in 1984 and 1986, respectively. He was awarded his Ph.D. in nuclear physics at University of Massachusetts at Amherst, Massachusetts, USA, in 1993. He has played an important role in developing Resistive Plate Chambers (RPCs) for the Compact Muon Solenoid (CMS) experiment of the Large Hadron Collider (LHC) at CERN, Switzerland. He is also working on development of the Large Acceptance Multi-Purpose Spectrometer (LAMPS) for frontier nuclear physics researches with rare isotopes at RAON. He is a member of the Korea Physical Society.